THE ASTROPHYSICAL JOURNAL, 493:519–522, 1998 February 1

EXPECTATIONS FOR THE DIFFERENCE BETWEEN LOCAL AND GLOBAL MEASUREMENTS OF THE HUBBLE CONSTANT

XIANGDONG SHI
Department of Physics, University of California, La Jolla, CA 92093-0319; shi@doheny.ucsd.edu

AND

MICHAEL S. TURNER
Departments of Astronomy & Astrophysics and of Physics Enrico Fermi Institute, University of Chicago, Chicago, IL 60637-1433; NASA/Fermilab Astrophysics Center, Fermi National Accelerator Laboratory, Batavia, IL 60510-0500; mturner@oddjob.uchicago.edu
Received 1997 July 8; accepted 1997 September 10

ABSTRACT

There are irreducible differences between the Hubble constant measured locally and the global value. They are due to density perturbations, a finite sample volume (cosmic variance), and a finite number of objects in the sample (sampling variance). We quantify these differences for a suite of *COBE*-normalized cold dark matter models that are consistent with the observed large-scale structure. For small samples of objects that only extend to 10,000 km s^{-1}, the variance can approach 4%. For the largest samples of Type Ia supernovae (SNe Ia), which include about 40 objects and extend to almost 40,000 km s^{-1}, the variance is 1%–2% and is dominated by sampling variance. Sampling and cosmic variance may be an important consideration in comparing local determinations of the Hubble constant with precision determinations of the global value that will be made from high-resolution maps of cosmic background radiation anisotropy.

Subject headings: cosmic microwave background — cosmology: observations — cosmology: theory — distance scale

1. INTRODUCTION

On the largest scales ($\gtrsim 100$ Mpc), the universe is well described by homogeneous and isotropic expansion that satisfies the Friedmann equation. The global rate of expansion at the current epoch is defined to be the Hubble constant ($\equiv H_0$), the fundamental parameter of cosmology that sets the size and age of the universe. Many methods have been used to measure H_0 (see, e.g., Freedman 1997). Currently, the use of Type Ia Supernovae (SNe Ia) as standard candles yields the smallest estimated measurement error (Riess, Press, & Kirshner 1996; Hamuy et al. 1996; Saha et al. 1996).

On small scales ($\lesssim 100$ Mpc), the universe is significantly inhomogeneous. Because density fluctuations give rise to deviations from isotropic and homogeneous expansion (peculiar velocities), the expansion cannot be characterized by a universal expansion rate and measurements within a small, finite region will yield a local expansion rate ($\equiv H_L$) that is not identical to the global expansion rate. The difference arises from two factors: (1) the finite physical size of the sample (Turner, Cen, & Ostriker 1992; Nakamura & Suto 1995; Shi, Widrow, & Dursi 1996; Turner 1997) and (2) the limited number of objects in the sample. Because of peculiar velocities, the average expansion rate in a finite volume is different from the global expansion rate (cosmic variance). Moreover, because only a small number of points within the volume are sampled, the expansion rate defined by these points can deviate from the average expansion rate for the volume (sampling variance). These effects are different from measurement error, which can be reduced by better measurements and/or better standard candles. Cosmic and sampling variance can only be reduced by increasing the sample volume and the sampling density.

In this paper, we quantify cosmic and sampling variance for two samples of SNe Ia and a cluster sample with Tully-Fisher distances. In doing so, we use a suite of *COBE*-normalized cold dark matter (CDM) models that are consistent with the measurements of the level of inhomogeneity on scales less than about 300 Mpc, which should provide a reasonable estimate for the variance that arises due to inhomogeneity in the universe.

2. METHODOLOGY

The deviation of the local expansion rate measured by an observer at position $\boldsymbol{r}$ from the global Hubble constant is given by

$$\frac{H_L(\boldsymbol{r}) - H_0}{H_0} = \frac{\delta H(\boldsymbol{r})}{H_0} = \int \frac{\boldsymbol{v}(\boldsymbol{r}' - \boldsymbol{r}) \cdot (\hat{\boldsymbol{r}}' - \hat{\boldsymbol{r}})}{H_0 |\boldsymbol{r} - \boldsymbol{r}'|} W(\boldsymbol{r}' - \boldsymbol{r}) d^3 r' , \quad (1)$$

where $\boldsymbol{v}(\boldsymbol{r}' - \boldsymbol{r}) \cdot (\hat{\boldsymbol{r}}' - \hat{\boldsymbol{r}})$ is the measured radial peculiar velocity at $\boldsymbol{r}'$ and $W(\boldsymbol{r}' - \boldsymbol{r})$ is the window function that characterizes the sample volume and sampled points within the volume (more below). The quantity $\boldsymbol{v}(\boldsymbol{r}' - \boldsymbol{r}) \cdot (\hat{\boldsymbol{r}}' - \hat{\boldsymbol{r}})$ consists of two parts, the actual radial peculiar velocity and its measurement error, which is roughly the measurement error of the distance scaled by H_0. The measurement error can be shrunk by improving distance measurements, but the real radial peculiar velocity is an intrinsic deviation from the Hubble flow that is determined by the underlying density fluctuations. It is its contribution to $\delta H(\boldsymbol{r})/H_0$ that is irreducible.

The peculiar velocity field depends upon the underlying power spectrum of density perturbations, which in turn depends upon the cosmological scenario. We shall investi-

gate a number of CDM models. In linear perturbation theory,

$$\boldsymbol{v}(\boldsymbol{r}) = \frac{H_0 \Omega_M^{0.6}}{2\pi} \int \frac{\boldsymbol{r} - \boldsymbol{r}'}{|\boldsymbol{r} - \boldsymbol{r}'|^3} \, \delta(\boldsymbol{r}') d^3 r' \tag{2}$$

where $\delta(\boldsymbol{r}')$ is the density fluctuation $[\rho(\boldsymbol{r}') - \bar{\rho}]/\bar{\rho}$ and Ω_M is the fraction of critical density in matter that clusters. Taking the Fourier transform, we find

$$\frac{\delta H(\boldsymbol{r})}{H_0} = \Omega_M^{0.6} \int \frac{d^3 k}{(2\pi)^{3/2}} \, \delta(\boldsymbol{k}) \, \frac{\boldsymbol{k} \cdot \boldsymbol{Z}(\boldsymbol{k})}{k^2} \, e^{i\boldsymbol{k} \cdot \boldsymbol{r}} \, , \tag{3}$$

where $\delta(\boldsymbol{k}) \equiv (2\pi)^{-3/2} \int d^3 r \, \delta(\boldsymbol{r}) e^{i\boldsymbol{k} \cdot \boldsymbol{r}}$ and $\boldsymbol{Z}(\boldsymbol{k}) \equiv \int d^3 r \, W(\boldsymbol{r})(\hat{\boldsymbol{r}}/r) e^{i\boldsymbol{k} \cdot \boldsymbol{dr}}$. The variance of $\delta H(\boldsymbol{r})/H_0$ is

$$\left\langle \left(\frac{\delta H}{H_0} \right)^2 \right\rangle^{1/2} = \Omega_M^{1.2} \int \frac{d^3 k}{(2\pi)^3} \, \frac{P(k)}{k^2} \, |\boldsymbol{Z}(\boldsymbol{k}) \cdot \hat{\boldsymbol{k}}|^2 \, . \tag{4}$$

For a top-hat, spherical window function,

$$\boldsymbol{Z}(\boldsymbol{k}) = 3 \, \frac{\sin\,(kR) - \int_0^{kR} dx \, \sin\,(x)/x}{(kR)^3} \, \boldsymbol{k} \, , \tag{5}$$

where $W(\boldsymbol{r}' - \boldsymbol{r}) = \Theta(R - |\boldsymbol{r}' - \boldsymbol{r}|)/(4\pi R^3/3)$, $\Theta(x)$ is the step function and R is the radius of the top-hat sphere (Shi et al. 1996). Since the top-hat spherical window function samples every point within the sphere, $\langle [\delta H(\boldsymbol{r})/H_0]^2 \rangle^{1/2}$ reflects only the cosmic variance associated with the finite volume of the spherical sample.

Real data sets do not sample every point in space, rather they sample a number of objects with positions $\boldsymbol{r}_q$ and redshifts z_q. The radial peculiar velocities of these objects are

$$\boldsymbol{v}_q \cdot \hat{\boldsymbol{r}}_q = c z_q - H_0 r_q \, , \tag{6}$$

with uncertainties σ_q that are essentially the uncertainties in distances r_q scaled by H_0 because the uncertainties in z_q are relatively small. Random motions due to local nonlinearities, characterized by a one-dimensional standard velocity dispersion σ_*, may be added to σ_q in quadrature. Typically $\sigma_* \sim 10^2$ km s^{-1}, and is therefore negligible when the sample depth is as large as $\sim 10^4$ km s^{-1}. Corrections to the linear Hubble law due to deceleration can also be safely ignored for samples with $z \ll 1$. With these approximations, it follows that (Shi 1997)

$$Z^i(\boldsymbol{k}) = B^{-1} \Bigg[\sum_q \frac{r_q^i}{\sigma_q^2} \, e^{i\boldsymbol{k} \cdot \boldsymbol{r}_q} - (A - RB^{-1})^{-1}_{jl} \times \left(\sum_q \frac{\hat{r}_q^i \hat{r}_q^j}{\sigma_q^2} \, e^{i\boldsymbol{k} \cdot \boldsymbol{r}_q} - B^{-1} \sum_q \sum_{q'} \frac{r_q^i r_{q'}^j}{\sigma_q^2 \sigma_{q'}^2} \, e^{i\boldsymbol{k} \cdot \boldsymbol{r}_q} \right) \sum_{q''} \frac{r_{q''}^l}{\sigma_{q''}^2} \Bigg] , \tag{7}$$

where

$$A_{ij} = \sum_q \frac{\hat{r}_q^i \hat{r}_q^j}{\sigma_q^2} \, , \quad R_{ij} = \sum_q \sum_{q'} \frac{r_q^i r_{q'}^j}{\sigma_q^2 \sigma_{q'}^2} \, , \quad B = \sum_q \frac{r_q^2}{\sigma_q^2} \, , \tag{8}$$

indices q, q', and q'' denote summation over objects, and indices i, j, l, m are spatial indices that run from 1 to 3. Now $\langle [\delta H(\boldsymbol{r})/H_0]^2 \rangle^{1/2}$ includes both cosmic variance and sampling variance.

3. RESULTS

Using equations (1)–(5), we have calculated the cosmic variance portion of $\langle [\delta H(\boldsymbol{r})/H_0]^2 \rangle^{1/2}$ with $R = 7000$, 10,000, 15,000, 20,000, 25,000, and 30,000 km s^{-1} (see Fig. 1). The underlying cosmological models are a suite of *COBE*-normalized CDM models that are consistent with large-scale structure on scales from about 300 Mpc to 0.1 Mpc (Dodelson, Gates, & Turner 1996). The CDM models include a model with a low value of the Hubble constant, significant tilt, 20% light neutrinos, additional radiation, and a cosmological constant. In addition, we have included an open CDM model that is consistent with large-scale structure measurements and, for completeness, a standard CDM model that has excessive inhomogeneity on scales less than 300 Mpc. These models should serve well to span theoretical expectations for the level of inhomogeneity on the scales relevant for local variations in the Hubble constant. Their cosmic parameters are summarized in Table 1.

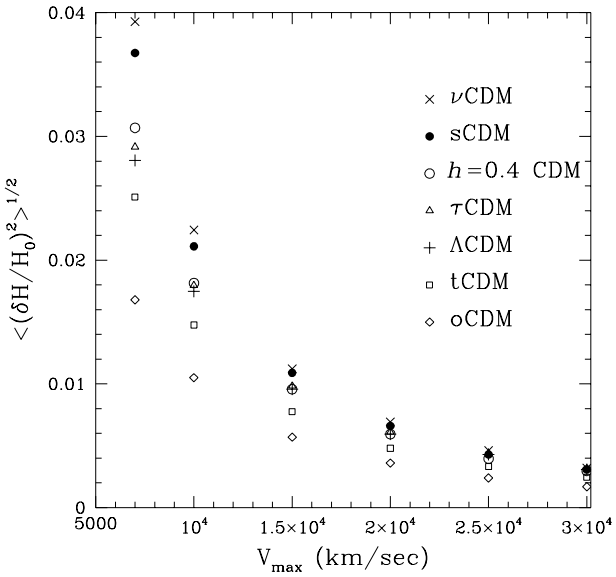

FIG. 1.—Cosmic variation as a function of the radius of the sample volume for the seven *COBE*-normalized CDM models.

The cosmic variance of H_L at $R = 7000$ km s^{-1} is significant, ranging from about 2% to almost 4%. At $R = 10{,}000$ km s^{-1}, it falls to 1%–2%, and quickly declines to below 1% at $R = 15{,}000$ km s^{-1} for all models. At a depth of $R = 30{,}000$ km s^{-1}, which is reached by SNe Ia, the cosmic variance is only about 0.2%.

Using equation (8), we have calculated $\langle [\delta H(\boldsymbol{r})/H_0]^2 \rangle^{1/2}$ for volumes that are sampled by a finite number of points so that both cosmic and sampling variance are included. For definiteness we use the SN Ia sample of Riess et al. (1997, private communication) for which $H_L = 65$ km s^{-1} Mpc^{-1}; the SN Ia sample of Hamuy et al. (1996) for which $H_L = 63.1 \pm 3.4 \pm 2.9$ km s^{-1} Mpc^{-1}); and the Tully-Fisher sample of 36 clusters used for the template Tully-Fisher relation in the Mark III catalog (Willick et al. 1997). Our results are compiled in Table 2.

The intrinsic variance of H_L measured in the two SN Ia samples is around 1%, far less than measurement error. Although the SN Ia sample of Riess et al. (1997, private communication) is deeper and has more objects than that of Hamuy et al. (1996), its effective depth is not as large because many of the SNe Ia are nearby. Due to its shallow depth, the Tully-Fisher cluster sample has a larger intrinsic variance, between 1.5% and 3%.

Figure 2 illustrates the effect of finite sampling for the SN Ia sample of Riess et al. (1997, private communication). Comparing this plot to Figure 1, it can be seen that the

TABLE 1

PARAMETERS OF SEVEN CDM MODELS[a]

	sCDM	$h = 0.4$ CDM	tCDM	νCDM	τCDM	ΛCDM	oCDM
Ω_{TOT}.....	1	1	1	1	1	1	0.4
Ω_M	1	1	1	1	1	0.4	0.4
Ω_B	0.1	0.16	0.08	0.07	0.08	0.06	0.07
Ω_ν	0	0	0	0.2	0	0	0
h	0.5	0.4	0.55	0.6	0.55	0.65	0.6
n	1	1	0.7	1	0.95	1	1.1

[a] CDM models from Dodelson et al. 1996. Their power spectra are based upon Bardeen et al. 1986 (transfer function), Bunn & White 1997 (*COBE* normalization), Sugiyama 1995 (effect of Ω_B on transfer function), and Ma 1996 (νCDM transfer function). The oCDM model is White & Silk 1996. With the exception of standard CDM, which is included only for completeness, all models are consistent with measures of large-scale structure on scales from 300 Mpc to 0.1 Mpc.

cosmic + sampling variance is more than twice the cosmic variance. At present, sampling variance dominates the intrinsic variance for the SN Ia samples. Since sampling variance scales roughly as the inverse square root of the number of objects, it can be shrunk to less than 1% for all viable CDM models, if the number of SNe Ia is doubled.

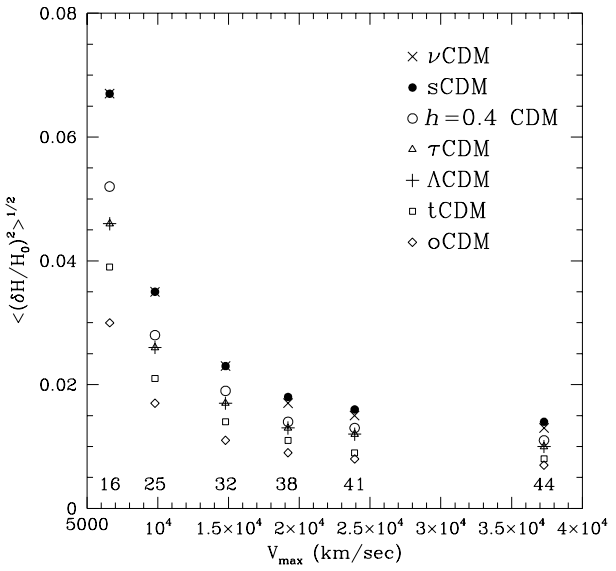

FIG. 2.—Cosmic + sampling variance for the SN Ia sample of Riess et al. (1997). The numbers indicate the number of objects within the spherical sample volume.

4. SUMMARY

There are intrinsic and irreducible differences between the locally measured value of the Hubble constant and the global value. They arise due to finite sample volume (cosmic variance) and finite sample size (sampling variance) and can of course be of either sign. Cosmic variance and sampling variance cannot be reduced by better measurements or better standard candles.

We have calculated the theoretical expectations for a suite of *COBE*-normalized CDM models that are consistent with measurements of large-scale structure on the scales that give rise to the cosmic variance portion. For samples that only extend to 7000 km s^{-1}, the cosmic variance alone can be close to 4%; for samples of around 30 objects that extend to 10,000 km s^{-1}, cosmic + sampling variance is between 2% and 4%. For samples of around 40 objects that extend out to 40,000 km s^{-1}, the total variance is between 0.5% and 1.5%, with the cosmic variance contribution being less than 0.25%.

As local measurements of the Hubble constant become more precise, cosmic variance and sampling variance will become a larger portion of the error budget and may be important when comparing local measurements with the better than 1% determinations of the Hubble constant

TABLE 2

COSMIC + SAMPLING VARIANCE FOR THREE SAMPLES.

Parameter/Model	SNe Ia (Riess et al. 1997, private communication)	SNe Ia (Hamuy et al. 1996)	Tully-Fisher (Willick et al. 1997)
	Model Parameters		
Maximal depth (km s^{-1}).....	37,000	30,000	11,000
$\pi H_0/k_{peak}$[a](km s^{-1})	~21,000	~27,000	10,000
Number of objects.....	44	26	36
	Variance (%)		
sCDM.....	1.4	1.4	3.1
$h = 0.4$ CDM	1.1	1.1	2.6
τCDM	1.0	0.9	2.3
νCDM	1.3	1.3	3.1
tCDM.....	0.8	0.8	1.8
ΛCDM.....	1.0	0.9	2.4
oCDM	0.7	0.6	1.6

[a] k_{peak} is the wavenumber where $|\boldsymbol{Z}(\boldsymbol{k}) \cdot \hat{\boldsymbol{k}}|^2$ reaches maximum.

anticipated from high-resolution maps of CBR anisotropy (Jungman et al. 1996).

The authors thank Adam Riess for providing the positions of their unpublished SNeIa. X. S. is supported by NASA grant NAG 5-3062 and NSF grant PHY 95-03384 at the University of California, San Diego. M. S. T. is supported by DoE (at the University of Chicago and Fermilab) and by NASA grant NAG 5-2788 at Fermilab.

REFERENCES

Bardeen, J. M., Bond, J. R., Kaiser, N., & Szalay, A. S. 1986, ApJ, 304, 15
Bunn, E. F., & White, M. 1997, ApJ, 480, 6
Dodelson, S., Gates, E., & Turner, M. S. 1996, Science, 274, 69
Freedman, W. 1997, in Critical Dialogues in Cosmology, ed. N. Turok (Singapore: World Scientific)
Hamuy, M., et al. 1996, AJ, 112, 2398
Jungman, G., Kamionkowski, M., Kosowsky, A., & Spergel, D. N. 1996, Phys. Rev., 54, 1332
Ma, C. 1996, ApJ, 471, 13
Nakamura, T. T., & Suto, Y. 1995, ApJ, 447, L65
Saha, A., et al. 1996, ApJS, 107, 693
Shi, X. 1997, ApJ, 486, 32
Shi, X., Widrow, L. M., & Dursi, L. J. 1996, MNRAS, 281, 565
Sugiyama, N. 1995, ApJS, 100, 281
Turner, E. L., Cen, R., & Ostriker, J. P. 1992, AJ, 103, 1427
Turner, M. S. 1997, in The Extragalactic Distance Scale, ed. M. Livio, M. Donahue, & N. Panagia (Cambridge: Cambridge Univ. Press), 6
Riess, A. G., Press, W. H., & Kirshner, R. P. 1996, ApJ, 473, 88
White, M., & Silk, J. 1996, Phys. Rev. Lett., 77, 4704
Willick, J., et al. 1997, ApJS, 109, 333